Automatica, Vol. 39, 2003, pp. 1461–1467

# Semi-Intrusive Multivariable Model Invalidation [1]

Leonardo C. Kammer [a,*] Dimitry Gorinevsky [b]
Guy A. Dumont [a]

[a] *Pulp and Paper Centre, University of British Columbia, 2385 East Mall, Vancouver, BC V6T 1Z4, Canada*

[b] *Honeywell Global Control Laboratory, One Results Way, Cupertino, CA 95014, U.S.A.*

**Abstract**

This paper introduces a mechanism for testing multivariable models employed by model-based controllers. Although external excitation is not necessary, the data collection includes a stage where the controller is switched to open-loop operation (manual mode). The main idea is to measure a certain "distance" between the closed-loop and the open-loop signals, and then trigger a flag if this "distance" is larger than a threshold level. Moreover, a provision is made for accommodating model uncertainty. Since no hard bounds are assumed with respect to the noise amplitude, the model invalidation mechanism works in a probabilistic framework.

*Key words:* Model invalidation; performance monitoring; model-based control; multivariable control systems; stochastic noise; model uncertainty.

## 1 Introduction

Advanced multivariable controllers in process industries are typically model-based predictive control algorithms implemented as proprietary software. Most of the commercially available controllers allow a user to access process data and models, but not the details of the controller design. Hence, a practical

* Corresponding author. Current address: Paprican, 3800 Wesbrook Mall, Vancouver, BC V6S 2L9, Canada. Fax: +1 604 222-3207. E-mail: lkammer@paprican.ca

[1] The original version of this paper was presented at ECC 2001, which was held in Porto, Portugal during September 2001.

performance monitoring method ought not to rely on detailed knowledge of the controller itself.

If the process suffers an upset resulting in suboptimal operation of the plant, it is important to know whether the problem is caused by process disturbances or by an error in the process model used by the controller. A typical operator reaction is to put some supervisory control loops in manual mode, wait and see if the process variables settle down. These data, collected in open loop, can be used for testing the model. Problems related to a bad model could be fixed by re-identifying the entire multivariable model and re-tuning the controller. However, this is a very expensive procedure and it should not be undertaken unless there is certainty about the existing model being a problem.

Our goal is to provide a signal processing mechanism that deals with the scenario described above to reveal if the model embedded in the controller is no longer valid. Moreover, the mechanism shall indicate which part of the multivariable model is wrong, so that only that part of the model needs to be re-identified. The worst-case scenario is assumed: the only data available from the system are collected after the problem has been detected and no measurable external excitation occurs during data collection. That is, the only excitation driving the loop come from stationary stochastic process disturbances.

Traditional mechanisms of "model validation" (Ljung, 1999) use high excitation not only to falsify the estimated model, but also to gain confidence on a model that passes the test. In contrast we use the term "model invalidation" to characterize simple tests, with little or no excitation, that put the plant model on trial without aiming at increasing the confidence on this model.

The mechanisms for performance monitoring are the ones best suited for achieving model invalidation. These excitation-free mechanisms are dedicated to analyzing the loop performance with respect to a specific criterion like minimum variance (Harris, 1989), or to a specific problem like valve stiction (Hägglund, 1995; Horch, 1999) or sluggish control (Hägglund, 1999). In our problem, the loop performance is not described by a single numerical index and we also wish to account for a certain degree of uncertainty in the model.

The mechanism introduced in this paper compares two sets of data (time series) associated with each output: the model output error $(y(t) - \hat{y}(t))$, collected during normal operation, and the open-loop output, collected when the controller is put in manual. In Section 2 it is shown that if the process model is correct and the disturbance is stationary, then those two time series present the same behaviour. Thus, we need a tool that quantifies the "distance" between the behaviour of two independent time series. Section 3 develops such a tool, in a probabilistic framework, along with a threshold value for rejecting the

hypothesis that part of the model is correct. Given that in real-life modelling errors are always present, Section 4 extends the mechanism to accommodate for uncertainties in the closed-loop response. A simulation example is presented in Section 5, where the "actual plant" is modified to test the behaviour of the invalidation mechanism.

## 2 Model Output Error

The scenario analyzed in this work is restricted to plants with unmeasurable sources of stochastic noise:

$$y(t) = G(q)\,u(t) + H(q)\,e(t), \tag{1}$$

where $y(t)$ is the vector of $n_y$ output signals, $u(t)$ is the vector of $n_u$ input signals and $\{e(t)\}$ is a vector of $n_e$ independent zero-mean Gaussian white-noise processes. The transfer-function matrices $G(q)$ and $H(q)$ have dimensions $n_y \times n_u$ and $n_y \times n_e$, respectively. $G(q)$ must be stable, but $H(q)$ may contain poles at $z = 1$.

The control action is also restricted to minimal excitation (constant reference signals). This leads to the following structure for the control action:

$$u(t) = -C(q)\,y(t). \tag{2}$$

$C(q)$ is an unknown operator designed from a known model of the process:

$$\hat{y}(t) = \hat{G}(q)\,u(t). \tag{3}$$

From (1) and (3) we define the model output error as

$$\begin{aligned} \varepsilon(t) &\triangleq y(t) - \hat{y}(t) \\ &= [G(q) - \hat{G}(q)]\,u(t) + H(q)\,e(t) \\ &= [I + \hat{G}(q)C(q)][I + G(q)C(q)]^{-1}H(q)\,e(t). \end{aligned} \tag{4}$$

These expressions show that if the model is perfect ($\hat{G}(q) \equiv G(q)$) then the model output error presents the same dynamics as the process noise, $H(q)\,e(t)$. This fact is essential to our mechanism, as we compare two time series for each process output: the model output error, $\varepsilon(t)$, and the open-loop output signal,

$$y^o(t) = H(q)\,e(t). \tag{5}$$

It is imperative that the noise dynamics, $H(q)$, be time invariant, at least for the duration of the experiment. Although in practice this assumption might

not always hold, the development of a mechanism to test this assumption is beyond the scope of the paper. As a minimal practical check, the user can collect data in the following sequence: normal operating data, open-loop data, normal operating data; and compare the noise dynamics in both regions of closed-loop data.

The invalidation test thus becomes a trial of the assumption that, for each process output $j = 1, \ldots, n_y$, the time series $\{\varepsilon_j(t)\}$ and $\{y_j^o(t)\}$ are realizations of the same stationary process. If $H(q)$ contains poles at $z = 1$, then both time series must be differenced an appropriate amount of times for $\{y_j^o(t)\}$ to become stationary (Box *et al.*, 1994).

A closer look at the centre line in (4) reveals that, in principle, the test is completely independent on the type of controller being used. That is, the controller could be nonlinear, time-variant, etc. Nevertheless, under this wider scenario the conclusions about the loop uncertainty are no longer valid. This also applies when the reference signals are not constant. That is, changes in the reference signals would emphasize existing plant-model mismatches, affecting the uncertainty analysis presented here.

## 3 Comparison of Two Time Series

The problem statement addressed in this section is: *Given two independent time series,* $\{z_1(t)\}$ *and* $\{z_2(t)\}$*, test the assumption that they are realizations of the same stationary process.*

This problem has been considered before and several solutions were proposed in the literature, both in the time domain (Quenouille, 1958; Pudney *et al.*, 1999) and the frequency domain (Coates and Diggle, 1986; Diggle and Fisher, 1991). Another distinction between these solutions is whether they are parametric or nonparametric. Analyses consistently conclude that the parametric methods are more powerful, in the sense of being able to detect smaller differences in the time series (Coates and Diggle, 1986; Diggle and Fisher, 1991). On the other hand, the nonparametric methods are simpler as they do not require building an auxiliary parametric model of the series.

Herein we propose a frequency-domain method based on the work by Coates and Diggle (1986). This solution has immediate connection with the frequency-domain characterization of loop uncertainty. The method of Coates and Diggle is modified in our work to improve its power. Instead of deriving the probability distribution of the periodogram ordinates, we start by smoothing the periodogram and then derive the corresponding distributions.

### 3.1 Smoothed Periodogram

The periodogram of a time series $\{z_1(t)\}$ of length $N$ is the set of $m = \lfloor (N-1)/2 \rfloor$ values

$$I_1(\omega_k) = (2\pi N)^{-1} \left| \sum_{t=1}^{N} z_1(t)\ \mathrm{e}^{-i\omega_k t} \right|^2, \tag{6}$$

where $\omega_k = 2\pi k/N$, $k = 1, \ldots, m$. It is assumed that the process generating $\{z_1(t)\}$ is a stationary general linear process with independent identically distributed innovations. Therefore, asymptotically, $2I_1(\omega)/\,\mathrm{E}\{I_1(\omega)\}$ has a chi-squared distribution with two degrees of freedom and, for $l \neq k$, $I_1(\omega_l)$ and $I_1(\omega_k)$ are independent (Jenkins and Watts, 1968). It is important to emphasize that $I_1(0)$ and $I_1(\pi)$ are excluded since their sampling distribution are proportional to $\chi_1^2$ rather than $\chi_2^2$ (Coates and Diggle, 1986).

At this point our analysis deviates from that of (Coates and Diggle, 1986) as we smooth the periodogram. Actually, prior to smoothing the periodogram it is important to reduce large differences in amplitude at the various frequencies. That is, one of the two time series is whitened, then the same whitening filter, $W(q)$, is used on the other time series. The whitening is performed by fitting an auto-regressive model of low order to the time series, which is then filtered through the inverse of this model (a moving average filter). This whitening/filtering automatically differences the time series an appropriate amount of times in those situations where $H(q)$ contains poles at $z = 1$. The order of the auto-regressive model is increased until the filtered time series passes a whiteness test.

For our particular application, the time series containing the open-loop output signal, $\{y^o(t)\}$, is the natural choice for being initially whitened. For each output $j$, the signals to be compared are:

$$z_1(t) \triangleq W_j(q)\, y_j^o(t), \tag{7}$$

$$z_2(t) \triangleq W_j(q)\, \varepsilon_j(t). \tag{8}$$

Once the time series have been formed, their periodograms are smoothed via the convolution of a finite-length weight function (due to the special distribution of $I_1(0)$ and $I_1(\pi)$) and the frequency ordinates. Our choice of weight function is a triangular one,

$$\tilde{I}_1(\omega_k) = \sum_{j=-l+1}^{l-1} \lambda_j I_1(\omega_{k+j}), \quad k = l, \ldots, m-l+1 \tag{9}$$

$$\lambda_j = \frac{l - |j|}{l^2}, \tag{10}$$

which emphasizes the mid-frequencies relative to the fringes.

The length of the weight function reflects the type of mismatch we expect to detect between the periodograms $I_1(\omega)$ (of (7)) and $I_2(\omega)$ (of (8)). Mismatches that occur at a small frequency range are typical in closed-loop systems, therefore we adopt the following filter length:

$$l = \left\lfloor \frac{\sqrt{N}}{2} \right\rfloor. \tag{11}$$

Given $\tilde{I}_1(\omega)$ and $\tilde{I}_2(\omega)$, their difference at each frequency is measured by

$$J(\omega) \triangleq \ln \frac{\tilde{I}_1(\omega)}{\tilde{I}_2(\omega)}. \tag{12}$$

Notice that the order in which the time series are taken in (12) is important. The convention adopted in (7) and (8) implies that for scalar systems:

- a large positive value of $J(\omega_k)$ indicates that $|1 + \hat{G}(\mathrm{e}^{i\omega_k})C(\mathrm{e}^{i\omega_k})| \gg |1 + G(\mathrm{e}^{i\omega_k})C(\mathrm{e}^{i\omega_k})|$, that is, at frequency $\omega_k$ the Nyquist plot of $G(\mathrm{e}^{i\omega_k})C(\mathrm{e}^{i\omega_k})$ is closer to the critical point $-1$ than the designed Nyquist plot;
- a large negative value of $J(\omega_k)$ indicates that $|1 + \hat{G}(\mathrm{e}^{i\omega_k})C(\mathrm{e}^{i\omega_k})| \ll |1 + G(\mathrm{e}^{i\omega_k})C(\mathrm{e}^{i\omega_k})|$.

Loosely speaking, the former situation is associated with reduction of the stability margin, while the latter is associated with reduction of performance.

For multivariable systems one can take the absolute value of $J(\omega)$ and limit the analysis to the conclusion that large values imply a mismatch between designed and actual closed-loop behaviour.

### *3.2 The Threshold Level*

Asymptotically, $\nu\tilde{I}_1(\omega_k)/\,\mathrm{E}\{\tilde{I}_1(\omega_k)\}$ is approximately distributed as $\chi^2_\nu$ (Jenkins and Watts, 1968), where $\nu = 2/(\sum_{j=-l+1}^{l-1} \lambda_j^2)$, or more specifically, using (10), $\nu = 6l^3/(2l^2+1)$.

A very important characteristic of $J(\omega_k)$ is that if $\{z_1(t)\}$ and $\{z_2(t)\}$ are realizations of the same stationary process, then its (cumulative) distribution function depends only on $\nu$, and not on either $\omega_k$ or the original frequency distribution of the time series $\{y^o(t)\}$ and $\{\varepsilon(t)\}$ (due to the pre-whitening).

The cumulative distribution function is

$$F(J(\omega_k) < x) = \frac{\Gamma(\nu)}{\Gamma^2(\nu/2)} \int_{-\infty}^{x} \frac{\mathrm{e}^{\beta\,\nu/2}}{(1+\mathrm{e}^{\beta})^{\nu}} d\beta, \tag{13}$$

where $\Gamma(b)$ is the Gamma function. Expression (13) gives the probability that $J(\omega_k)$ at a particular frequency $\omega_k$ is less than a certain value $x$. In order to test the hypothesis that $\{z_1(t)\}$ and $\{z_2(t)\}$ are realizations of the same stationary process, we have to consider the set of $m - 2l + 2$ frequencies at which we smooth the periodogram:

$$J^* \triangleq \max_{\omega} |J(\omega)| \,. \tag{14}$$

If $\{z_1(t)\}$ and $\{z_2(t)\}$ are realizations of the same stationary process, then the distribution function of $J^*$ depends only on $N$; from this particular situation we derive the function $\zeta$:

$$\zeta(N,\alpha) \triangleq x \,|\, \mathrm{P}\{J^* \leq x \,|\, \mathrm{E}[\tilde{I}_1(\omega)] = \mathrm{E}[\tilde{I}_2(\omega)]\} = 1 - \alpha, \tag{15}$$

which provides the threshold level for testing the null hypothesis with significance level $\alpha$.

The analytical derivation of the threshold function $\zeta(N,\alpha)$ involves the computation of a large number of nested integrals, which is an extremely labour and computationally-intensive task. A reasonably accurate approximation of $\zeta$ can be computed via Monte Carlo simulations in a fraction of that effort. Table 1 provides some values of $\zeta$ obtained for several values of $N$ and two significance levels: 1% and 5%.

| $\zeta(N,\alpha)$ | | $N$ | | | | | |
|---|---|---|---|---|---|---|---|
| | | 300 | 400 | 500 | 750 | 1000 | 1500 |
| $\alpha$ | 0.01 | 1.57 | 1.39 | 1.34 | 1.25 | 1.17 | 1.05 |
| | 0.05 | 1.36 | 1.22 | 1.17 | 1.10 | 1.04 | 0.93 |

Table 1
Threshold levels for time series comparison

In summary, the hypothesis that $\{z_1(t)\}$ and $\{z_2(t)\}$ are realizations of the same stationary process is not rejected as long as $J^* \leq \zeta(N,\alpha)$. This test has a probability $\alpha$ of committing a Type I error (false alarm). Since this type of error should be avoided at all costs, $\alpha$ is typically a small value, e.g. 1%. Hence, any violations of the threshold $\zeta$ are attributed to model uncertainty.

## 4 Model Uncertainty

Consider the function $J(\omega)$ shown in Figure 1. The threshold level (dotted lines) is violated in both directions at frequencies assumed relevant for control purposes. Therefore it is helpful to characterize these violations in terms of closed-loop mismatch between actual and designed behaviour. The measure of threshold violation is computed frequency-by-frequency as

$$\gamma(\omega_k) \triangleq \begin{cases} J(\omega_k) - \zeta(N,\alpha) & \text{if } J(\omega_k) > \zeta(N,\alpha), \\ J(\omega_k) + \zeta(N,\alpha) & \text{if } J(\omega_k) < -\zeta(N,\alpha), \\ 0 & \text{otherwise.} \end{cases} \tag{16}$$

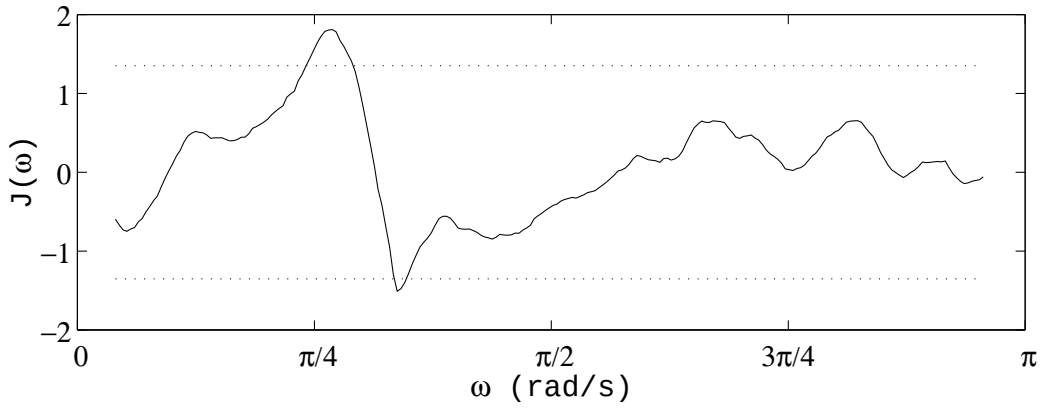


Fig. 1. Example of $J(\omega)$ (solid line) that violates the threshold at 1% significance level (dotted lines)

Whenever the processes generating $\tilde{I}_1(\omega)$ and $\tilde{I}_2(\omega)$ are different, we can express these quantities as $\tilde{I}_2(\omega) = \Delta(\omega)\,\hat{\tilde{I}}_1(\omega)$, where $\mathrm{E}[\hat{\tilde{I}}_1(\omega)] = \mathrm{E}[\tilde{I}_1(\omega)]$. Therefore, for $J(\omega_k) > \zeta(N,\alpha)$,

$$\begin{aligned} J(\omega_k) &= \ln \Delta(\omega_k) + \ln \frac{\hat{\tilde{I}}_1(\omega_k)}{\tilde{I}_1(\omega_k)} \\ &\leq \ln \Delta(\omega_k) + \max_{\omega} \ln \frac{\hat{\tilde{I}}_1(\omega)}{\tilde{I}_1(\omega)} \\ &\underset{\text{w.p. } 1-\frac{\alpha}{2}}{\leq} \ln \Delta(\omega_k) + \zeta(N,\alpha), \end{aligned} \tag{17}$$

where "w.p." stands for "with probability". The last step in (17) comes from (15) and the fact that the distribution of $\ln \frac{\hat{\tilde{I}}_1(\omega)}{\tilde{I}_1(\omega)}$ is symmetrical about zero. This leads to

$$\gamma(\omega_k) \underset{\text{w.p. } \geq 1-\frac{\alpha}{2}}{\leq} \ln \Delta(\omega_k). \tag{18}$$

That is, with a probability of at least $1 - \frac{\alpha}{2}$ we can conclude that the multiplicative discrepancy between $\tilde{I}_1(\omega_k)$ and $\tilde{I}_2(\omega_k)$ is at least as large as $\mathrm{e}^{\gamma(\omega_k)}$. Similar result is straightforwardly obtained when $J(\omega_k) < -\zeta(N, \alpha)$:

$$\gamma(\omega_k) \underset{\text{w.p. } \geq 1-\frac{\alpha}{2}}{\geq} \ln \Delta(\omega_k). \tag{19}$$

The connection between $\Delta(\omega)$ and model uncertainty is established for scalar systems. For these systems the following holds:

$$\begin{aligned} \lim_{N\to\infty} \mathrm{E}\left[\frac{\tilde{I}_2(\omega)}{\tilde{I}_1(\omega)}\right] &= \left|\frac{W[1+\hat{G}C][1+GC]^{-1}H}{WH}\right|^2 \\ &= \left|\frac{1+\hat{G}(\mathrm{e}^{i\omega})C(\mathrm{e}^{i\omega})}{1+G(\mathrm{e}^{i\omega})C(\mathrm{e}^{i\omega})}\right|^2 = \Delta(\omega), \end{aligned} \tag{20}$$

where $|1+\hat{G}(\mathrm{e}^{i\omega})C(\mathrm{e}^{i\omega})|$ gives the distance from the Nyquist plot of $\hat{G}(\mathrm{e}^{i\omega})C(\mathrm{e}^{i\omega})$ to the point $-1$. This distance, at each frequency, is part of the designed closed-loop behaviour, where a reduction in $|1+\hat{G}(\mathrm{e}^{i\omega})C(\mathrm{e}^{i\omega})|$ decreases the stability margin at that particular frequency and a move in the opposite direction tends to decrease the closed-loop performance. Hence we conclude, with a probability of at least $1 - \frac{\alpha}{2}$, that asymptotically the ratio between $|1+G(\mathrm{e}^{i\omega_k})C(\mathrm{e}^{i\omega_k})|$ and $|1+\hat{G}(\mathrm{e}^{i\omega_k})C(\mathrm{e}^{i\omega_k})|$ is at least as far from 1 as the value $\sqrt{\mathrm{e}^{-\gamma(\omega_k)}}$, at those frequencies where $\gamma(\omega_k) \neq 0$. Thus, as one can see, $\Delta(\omega)$ gives a characterization of a feedback loop gain uncertainty.

For multivariable systems the value of $\gamma(\omega)$ is affected by a combination of several transfer functions, instead of a single one ($G(\mathrm{e}^{i\omega})C(\mathrm{e}^{i\omega})$), and by the relative ratio between the amplitudes of the individual open-loop output signals. Consequently it is not as simple to interpret the function $\gamma(\omega)$ when we are dealing with more than one input or output.

It is left for the user to decide whether the closed-loop mismatch is within expectations given the uncertainty in the model. If one decides *a priori* the maximum acceptable mismatch in the closed-loop response, at each frequency, then the model invalidation test has all information needed to diagnose the loop and raise a flag whenever the maximum allowable mismatch is violated.

## 5 Simulation Example

As an example we perform a simulation analysis on the following $2 \times 2$ process of the form (1):

$$G(q) = \begin{bmatrix} g_{11} & g_{12} \\ g_{21} & g_{22} \end{bmatrix} = \begin{bmatrix} \frac{0.0315}{q^2-1.458q+0.479} & \frac{-0.025}{q^2-1.66q+0.688} \\ \frac{-0.09}{q^5-0.9q^4+0.2q^3} & \frac{-0.0385q+0.077}{q^2-1.54q+0.5785} \end{bmatrix},$$

$$H(q) = \begin{bmatrix} \frac{q^2-0.5q}{(q-1)(q-0.7)} & 0 \\ 0 & \frac{q^2-0.9q}{(q-1)(q-0.8)} \end{bmatrix}, \qquad \sigma_e^2 = \begin{bmatrix} 0.1 & 0 \\ 0 & 0.3 \end{bmatrix},$$

where $\sigma_e^2$ is the covariance matrix of the Gaussian white noise $e(t)$. A model $\hat{G}(q)$ is obtained as first-order plus time-delay approximations of the open-loop step responses of $G(q)$:

$$\hat{G}(q) = \begin{bmatrix} \frac{0.06}{q^2-0.96q} & \frac{-0.09}{q^3-0.9q^2} \\ \frac{-0.12}{q^5-0.6q^4} & \frac{0.1}{q^4-0.9q^3} \end{bmatrix}$$

Although the testing mechanism presented in this paper is aimed at model-predictive controllers, for simplicity we decided to use the following controller:

$$C(q) = \begin{bmatrix} \frac{5/6q^4-1.3q^3+0.48q^2}{d(q)} & \frac{0.6q^3-0.936q^2+0.3456q}{d(q)} \\ \frac{q^3-1.86q^2+0.864q}{d(q)} & \frac{0.4q^4-0.6q^3+0.216q^2}{d(q)} \end{bmatrix}$$

$$d(q) = q^4 - 2.0417q^3 + 0.6945q^2 + 0.9259q - 0.5787$$

This controller is designed such that $\hat{G}(q)C(q)$ is a diagonal transfer function matrix (full decoupling) with integral action in all channels and closed-loop step responses slightly faster then the diagonal elements of $\hat{G}(q)$. The actual closed-loop behaviour is fairly close to the designed one.

To investigate the probability of having the model invalidated by the proposed testing mechanism, we performed 1000 experiments applying the test as described in Section 3 with $\zeta(500, 0.01)$. Each simulation experiment comprises the following sequence of events:

- close the loop and wait for the signals to reach stationary behaviour;
- collect 500 points of $\varepsilon(t)$;
- open the loop;
- collect 500 points of $y^o(t)$.

From those 1000 experiments, 22 signalled problems at model output 1 and 16 experiments signalled problems at model output 2. The small mismatch between $G(q)$ and $\hat{G}(q)$ is responsible for this result since we expected to have about 10 experiments signalling problems at each model output.

Since we take the current model as acceptable, a region of model uncertainty is specified for this test: the maximum acceptable value for $|\gamma(\omega_k)|$ is $\ln|\Delta(\omega_k)| = 0.19$ (see Section 4). For a scalar system this value of $\gamma$ would asymptotically correspond to a Nyquist plot uncertainty in the range $[0.91, 1.10]$, at all frequencies. Under this condition another 1000 experiments were performed. As expected, the occurrences of model invalidations became very rare: two at model output 1 and zero at model output 2.

In order to test the efficacy of the model invalidation mechanism, we simulate an abrupt change in $g_{12}$ from the original $\frac{-0.025}{q^2-1.66q+0.688}$ to $\frac{-0.025}{q^6-1.66q^5+0.688q^4}$. This change has no observable influence on the variance of the plant outputs but increases the variance of the control movements $\Delta u_1$ and $\Delta u_2$ by approximately 25% and 50%, respectively. Another set of 1000 experiments is performed with the new system and the same uncertainty region as described above. The modelling error introduced in output 1 is successfully detected in 798 experiments and no invalidations occur of model output 2. Typical smoothed periodograms of the signals related to output 1 are shown in Figure 2, while Figure 3 shows the function $J(\omega)$ for output 1.

It is thus very likely that a single experiment realization will detect the problem in output 1. It remains to be found whether $\hat{g}_{11}$ or $\hat{g}_{12}$ is the main contributor to the model mismatch. A solution to this problem is to leave one control action active while freezing the other at a constant value (manual mode). After collecting these signals the role of each control action is inverted and new data are collected. These sets of signals are then analyzed against $y^o(t)$. For instance, when $u_2$ is active and $u_1 \equiv 0$, $\hat{g}_{11}$ and $\hat{g}_{21}$ are not excited, therefore plant/model mismatches can only be caused by either $\hat{g}_{12}$ or $\hat{g}_{22}$.

From those 798 experiments that signalled problems at model output 1, 673 of them continued to signal similar problems with $u_2$ active and $u_1 \equiv 0$, whereas 2 experiments also signalled the problem with $u_1$ active and $u_2 \equiv 0$. Another analysis shows that in these 2 cases the value of $J^*$ is larger when $u_2$ is active and $u_1 \equiv 0$, leading to the conclusion that $\hat{g}_{12}$ has a larger influence on the mismatch between $G(q)$ and $\hat{G}(q)$ than $\hat{g}_{11}$ does.

As a second investigation, a sinusoid was injected at output 1, with the process in its original value. The frequency of the sinusoid was chosen to be 0.4 rad/s, which is similar to the frequency where the peak of $J(\omega)$ is found in Figure 3. Under this sinusoidal disturbance, the variance of output 1 increases two times, the variance of output 2 remains the same, the variance of $\Delta u_1$ increases

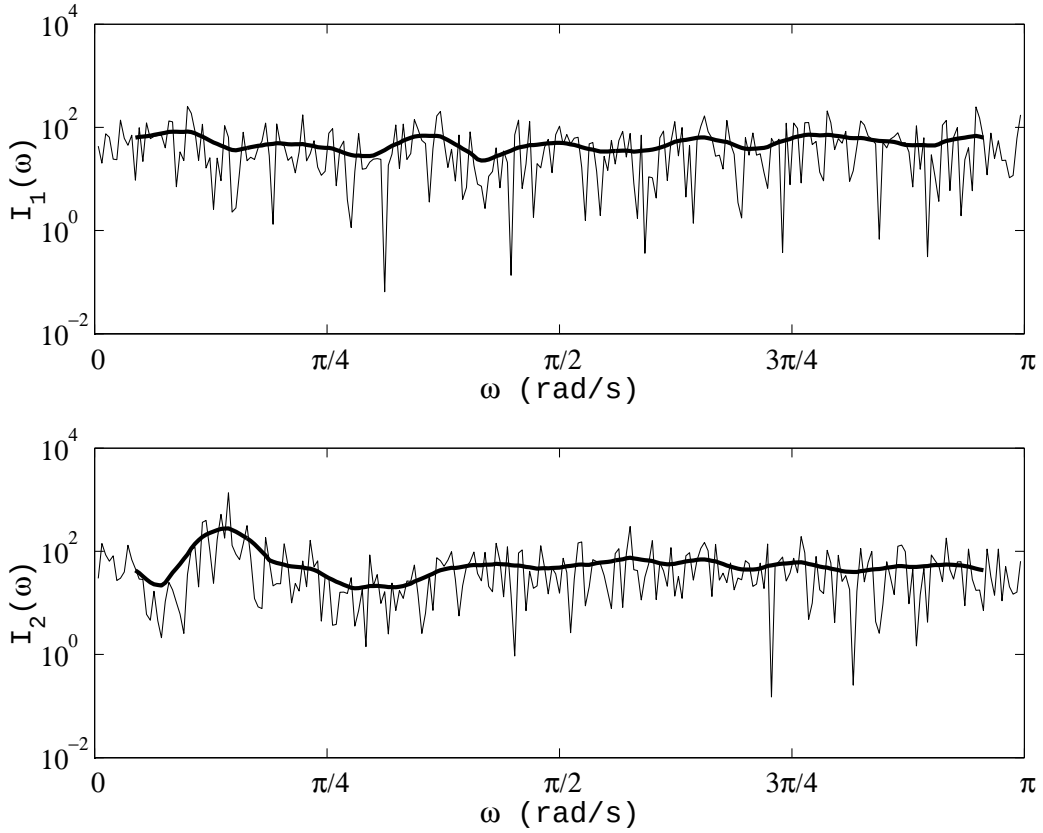


Fig. 2. Periodograms (thin lines) and their smoothed counterparts (thick lines) of $W_1(q)\, y_1^o(t)$ (top) and $W_1(q)\, \varepsilon_1(t)$ (bottom)

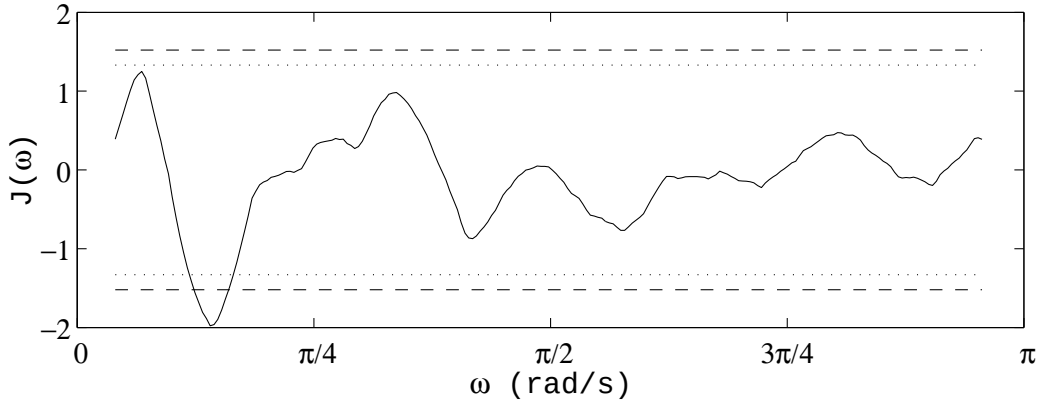


Fig. 3. Typical $J(\omega)$ of output 1 (solid line), as well as $\zeta(500, 0.01)$ (dotted lines) and the maximum allowable model uncertainty (dashed lines)

six times and the variance of $\Delta u_2$ increases nine times. 1000 experiments were performed under conditions identical to those described above, and no occurrences of model invalidation were observed at either output.

## 6 Conclusion

This article describes a novel approach to testing multivariable models employed in control systems design. The term "model invalidation" is used here to characterize simple tests, with little excitation, that put the plant model on trial. This is in sharp contrast to "model validation" tests, which apply high excitation in order to "prove" that the model is good. Our testing mechanism is well suited to the type of data readily available from industrial sites, especially when model-based predictive controllers are employed.

The test is based on the comparison of pairs of time series: one series is collected during normal closed-loop operation and the second one is collected under open-loop operation. This comparison provides means for assessing which model outputs are incorrect, but it remains to be identified which model inputs are problematic. A solution is provided in Section 5, where it is suggested that subsets of the controller outputs be inactive in order to test only parts of the model.

Similar to other mechanisms that extract information from measured data, like model identification and performance monitoring/assessment, deterministic load disturbances affect the final result. Periods with changes in load should be detected and excluded from the analysis.

The results obtained on simulation examples are very encouraging. Several aspects of the mechanism can be improved as the idea matures and new tests are performed. Ultimately, our goal is to have an automated tool for monitoring model-based controllers.

## References


Box, G. E. P., G. M. Jenkins and G. C. Reinsel (1994). *Time Series Analysis: Forecasting and Control*. third ed.. Holden-Day.

Coates, D. S. and P. J. Diggle (1986). Tests for comparing two estimated spectral densities. *Journal of Time Series Analysis* **7**(1), 7–20.

Diggle, P. J. and N. I. Fisher (1991). Nonparametric comparison of cumulative periodograms. *Applied Statistics* **40**(3), 423–434.

Hägglund, T. (1995). A control loop performance monitor. *Control Engineering Practice* **3**(11), 1543–1551.

Hägglund, T. (1999). Automatic detection of sluggish control loops. *Control Engineering Practice* **7**(12), 1505–1511.

Harris, T. J. (1989). Assessment of control loop performance. *The Canadian Journal of Chemical Engineering* **67**, 856–861.

Horch, A. (1999). A simple method for detection of stiction in process control loops. *Control Engineering Practice* **7**(10), 1221–1231.

Jenkins, G. M. and D. G. Watts (1968). *Spectral Analysis and its Applications*. Holden-Day. San Francisco, U.S.A.

Ljung, L. (1999). *System Identification: Theory for the User*. 2nd ed.. PTR Prentice Hall. Upper Saddle River, USA.

Pudney, S. E., D. F. Deadman and F. Clark (1999). A simple nonparametric test for the equality of autocorrelation structures of two stochastic processes, with application to experimental data. *Pub. Inst. Stat. Univ. Paris* **43**(2-3), 85–101.

Quenouille, M. H. (1958). The comparison of correlations in time-series. *Journal of the Royal Statistical Society* **20**(1), 158–164.